Proc. Natl. Acad. Sci. USA
Vol. 92, pp. 719–723, January 1995
Biochemistry

X-ray structure of a DNA decamer containing 7,8-dihydro-8-oxoguanine

(x-ray crystallography/DNA damage/oxidation/hydrogen bonding)

LEIGH ANN LIPSCOMB†, MARY ELIZABETH PEEK†, MARSHALL L. MORNINGSTAR‡, SUSAN M. VERGHIS‡§, ELIZABETH M. MILLER‡, ALEXANDER RICH¶, JOHN M. ESSIGMANN‡, AND LOREN DEAN WILLIAMS†‖

†School of Chemistry and Biochemistry, Georgia Institute of Technology, Atlanta, GA 30332-0400; and Departments of ‡Chemistry and ¶Biology, Massachusetts Institute of Technology, Cambridge, MA 02139

Contributed by Alexander Rich, October 4, 1994

ABSTRACT **We have determined the x-ray structure of a DNA fragment containing 7,8-dihydro-8-oxoguanine (G_O). The structure of the duplex form of d(CCAG$_O$CGCTGG) has been determined to 1.6-Å resolution. The results demonstrate that G_O forms Watson–Crick base pairs with the opposite C and that G_O is in the anti conformation. Structural perturbations induced by C·G$_O^{anti}$ base pairs are subtle. The structure allows us to identify probable elements by which the DNA repair protein MutM recognizes its substrates. Hydrogen bond donors/acceptors within the major groove are the most likely element. In that groove, the pattern of hydrogen-bond donors/acceptors of C·G$_O^{anti}$ is unique. Additional structural analysis indicates that conversion of G to G_O would not significantly influence the glycosidic torsion preference of the nucleoside. There is no steric interaction of the 8-oxygen of G_O with the phospho-deoxyribose backbone.**

Oxidative DNA damage contributes to rates of spontaneous mutation and may play a significant role in cancer and aging (1, 2). Oxidative DNA damage occurs when reactive oxygen species covalently damage DNA and cellular dNTP pools (3, 4) (reviewed in refs. 1, 5, and 6). An abundant form of oxidative damage is 7,8-dihydro-8-oxoguanine (G_O). G_O is formed by the reaction of singlet oxygen or hydroxyl radical either with guanine (G) in DNA or with dGTP. In DNA G is readily oxidized, so that 100,000 G_O DNA lesions are formed in an average mammalian cell per day (7).

When formed in DNA, G_O causes G → T transversions *in vivo* (8). During *in vitro* replication of template G_O within DNA, G_O pairs with both A and C (9). Polymerases involved in DNA replication (polymerases α, δ, and III) selectively incorporate A opposite template G_O, whereas polymerases involved in repair (polymerases I and β) selectively incorporate C. The proofreading activity of DNA polymerase I does not excise A incorporated opposite template G_O (9). However, the G_O·A mispair is proofread when G_O enters DNA from the precursor pool (10).

In *Escherichia coli*, at least three highly specific repair mechanisms reduce the mutagenic potential of G_O, underscoring the magnitude of the threat that oxidation poses to genetic integrity. The protein MutT removes dG$_O$TP from dNTP pools (11–13). On the DNA level, recognition of G_O base pairs appears to depend upon the composite structure of the covalent lesion and its pairing partner. The glycosylase MutM (14, 15), also known as formamidopyrimidine-DNA glycosylase (Fpg), acts on C·G$_O^{anti}$ base pairs (Fig. 1*B*). This glycosylase excises G_O, leading ultimately to restoration of normal C·G base pairs (Fig. 1*A*). By contrast, the base pair A·G$_O^{syn}$ (Fig. 1*C*) is a poor substrate for MutM (16). Another glycosylase, MutY (17–20), excises A from A·G$_O^{syn}$ base pairs as a first step in their conversion to C·G$_O^{anti}$ base pairs. MutM then completes the restoration of normal C·G base pairs. Two G_O repair enzymes have been identified in human cells (15, 21, 22), one with glycosylase activity and the other with endonuclease activity. Both of these enzymes excise G_O from DNA.

Oxidation of G to G_O has been thought to cause two significant structural changes in DNA and in dGTP. It is generally believed (23–25) that conversion from G to G_O switches the glycosidic torsion preference from anti to syn. This switch is thought to arise from steric repulsion between the 8-oxygen (O8) and deoxyribose. In addition, conversion from G to G_O alters the hydrogen bonding functionalities of the base. The 6,8-diketo form predominates at physiological pH (23). As shown in Fig. 1 *A–C*, oxidation of G converts the 7 position from a hydrogen bond acceptor to a donor and the 8 position from a very weak hydrogen bond donor to a strong hydrogen bond acceptor, O8. The arrangement of hydrogen bond donors/acceptors on the backside of G_O is *ada* (acceptor/donor/acceptor), the same as the pattern of hydrogen bond donors/acceptors of T. A preference for the syn conformation, coupled with the *ada* pattern of hydrogen bonding groups, is thought to be a primary feature causing G → T transversions by G_O. This model is supported by NMR studies with modified oligonucleotides (24, 25). The NMR data suggest that G_O resides in the anti conformation when paired with C (Fig. 1*B*), and in the syn conformation when paired with A (Fig. 1*C*). Base pairs between G$_O^{anti}$ and C are thought to be destabilized by steric repulsion that is only partially offset by hydrogen bonding interactions (as reviewed in refs. 5, 6, and 24).

We have determined the x-ray structure of a DNA fragment** containing G_O. The structure of the duplex form of d(CCAG$_O$CGCTGG) has been determined to 1.6-Å resolution. The results verify the C·G$_O^{anti}$ pairing scheme (Fig. 1*B*) but do not support destabilizing steric repulsion between O8 and deoxyribose. DNA structural perturbations induced by G_O are subtle. Our results and their implications for protein recognition of G_O are described here. We propose that hydrogen bonding properties of certain covalently modified purines provide a common recognition element among MutM substrates.

MATERIALS AND METHODS

DNA Synthesis. The decanucleotide containing G_O was prepared by the phosphoramidite procedure, starting from the deoxynucleoside 8-oxo-dG. The 8-oxo-dG was prepared from

The publication costs of this article were defrayed in part by page charge payment. This article must therefore be hereby marked "*advertisement*" in accordance with 18 U.S.C. §1734 solely to indicate this fact.

Abbreviations: G_O, 7,8-dihydro-8-oxoguanine.

§Present address: Department of Biology, Massachusetts Institute of Technology, Cambridge, MA 02139.
‖To whom reprint requests should be addressed.

**Atomic coordinates have been deposited in the Protein Data Bank, Chemistry Department, Brookhaven National Laboratory, Upton, NY 11973 (reference 183D). This information is not embargoed.

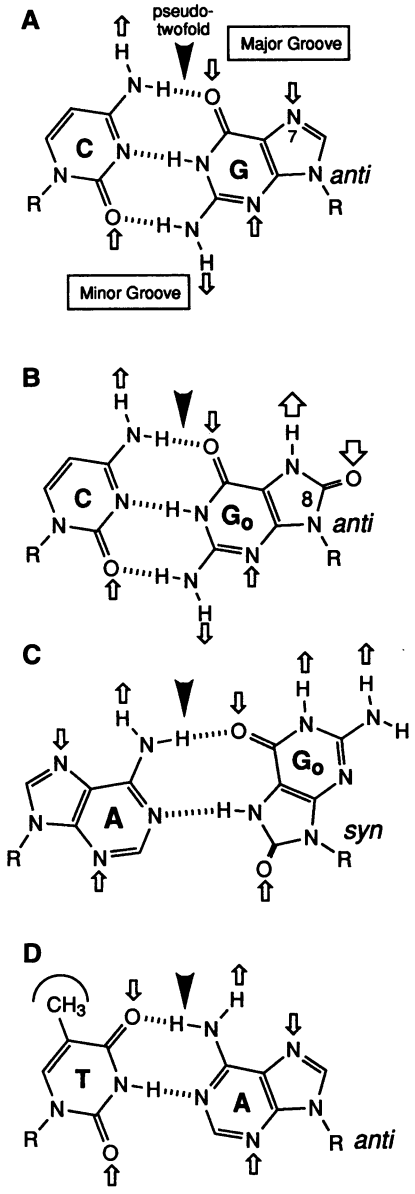

FIG. 1. (*A*) A normal C·G Watson–Crick base pair. The hydrogen bond donors and acceptors are indicated by open arrows. Arrows directed towards the base pair indicate hydrogen bond acceptors and arrows directed away from the base pair indicate hydrogen bond donors. The pseudo-twofold axis of the base pair is indicated by a solid arrow. (*B*) C·G_O^{anti} base pair. The large arrows indicate the hydrogen bond donor and acceptors that are common to many substrates of MutM. (*C*) A·G_O^{syn} base pair. (*D*) A·T base pair.

8-bromo-dG as described (26) except that reagent-grade dimethyl sulfoxide and higher temperatures (>100°C) were used. By this procedure 8-oxo-dG was directly obtained from 8-bromo-dG, eliminating one step in the synthesis. The crude 8-oxo-dG was subsequently peracylated with acetic anhydride in pyridine to yield triacetyl-8-oxo-dG (33% yield from 8-bromo-dG). Selective deprotection of the 5′ and 3′ hydroxyls with NaOH, protection of the 5′ hydroxyl with dimethoxytrityl (DMT) chloride, and activation of the 3′ hydroxyl with 2-cyano-*N,N*-diisopropyl chlorophosphoramidite were accomplished as described by Wood *et al.* (27). The 8-oxo-dG phosphoramidite was incorporated into d(CCAG$_O$CGCTGG) by solid-phase DNA synthesis on an Applied Biosystems 381A automated synthesizer. The 8-oxo-dG phosphoramidite was added manually. Similar to our results with the phosphoramidite of 7,8-dihydro-8-oxoadenine (27), the G_O phosphoramidite coupled only in low yields. Following oligonucleotide synthesis, the DMT-protected decamer was cleaved from the resin and the base-protecting groups were removed with concentrated NH_4OH (60°C, overnight). The DMT-oligonucleotide was subsequently purified by reversed-phase HPLC on a C_{18} column using elution with a linear gradient of 30–60% B (acetonitrile/0.1 M ammonium acetate, 1:1) in A (0.1 M ammonium acetate) over 50 min at a flow rate of 1 ml/min. The DMT group was removed according to Applied Biosystems User Bulletin 50 and the oligonucleotide was repurified by HPLC using a linear gradient of 0–20% B. The nucleotide composition was subsequently determined by enzymatic hydrolysis (27), reversed-phase HPLC, and UV detection of the digestion products. UV peak area analysis confirmed that the modified dodecamer contained the proper ratios of A, C, T, G, and G_O.

DNA Crystallization. Crystals of d(CCAG$_O$CGCTGG) were grown at 4°C from sitting drops containing 1.9 mM single-stranded DNA, 20 mM Tris·HCl (pH 7.6), 5% methylpentanediol, and 133 mM $MgCl_2$. The reservoir contained 30% methylpentanediol. No crystals appeared after 8 weeks at room temperature, at which time the setups were transferred to a 4°C cold room. After several months, chunky crystals appeared. The crystal used for data collection was 0.61 × 0.64 mm × 0.5 mm.

Data Collection. X-ray intensity data were collected at 4°C from a crystal in a glass capillary by a San Diego Multiwire Systems area detector and an Enraf–Nonius cryostat (model FR558SH). Copper Kα radiation (1.54 Å) was generated with a fine-focus Rigaku RU200 rotating anode. Data were collected in the ω scan mode. Unit-cell and space-group determination suggested that d(CCAG$_O$CGCTGG) was isomorphous with d(CCAGGCCTGG), solved previously (28). The space group of d(CCAG$_O$CGCTGG) is *C*2 and the unit cell dimensions are 32.27, 25.56, and 34.71 Å, β = 115.77°. Data collection and refinement statistics are presented in Table 1.

Refinement. The central residues of d(CCAGGCCTGG) (28) were switched from 5′-GC-3′ to 5′-CG-3′ with the program CHAIN (29). These coordinates, with a normal G at residue 4, were used as a starting model. After initial XPLOR [version 3.1 (30)] refinement of atomic coordinates and *B* values, the *R* factor was 29.5%. Even at this early stage of refinement, sum ($2F_o - F_c$) and difference ($F_o - F_c$) Fourier maps, calculated with XPLOR, clearly indicated the position of O8 of residue 4. Simulated annealing (XPLOR) decreased the *R* factor to 29.1%. The moderate decrease in *R* factor upon

Table 1. Data collection and refinement statistics

Resolution limit, Å	No. of reflections		*R* factor, %
	Collected	Possible	
3.17	443	447	21.0
2.53	431	434	23.0
2.21	430	430	24.4
2.01	418	418	24.8
1.87	418	418	25.4
1.76	431	433	23.7
1.67	414	417	26.1
1.60	241	389	28.7
(Total)	3290	3448	23.4

Total no. of observations:	12,930
No. of unique reflections ($I > 2\sigma$):	3,290
R_{merge} [$\Sigma\|(I_{avg} - I_{obs})\|/\Sigma(I_{avg})$]:	5.52%
rmsd of bond distances:	0.020 Å
rmsd of bond angles:	3.6°
Current *R* factor:	23.4%
Current asymmetric unit:	DNA decamer plus 42 waters

rmsd, Root-mean-square deviation from ideality.

simulated annealing reflects the accuracy of the starting model. Forty-three solvent molecules were added in groups of ≤10 from corresponding sum and difference electron density peaks. Conversion of residue G(4) to G_O(4) decreased the *R* factor by 0.3%. Addition of a hydrated magnesium ion and its surrounding water molecules is expected to significantly decrease the *R* factor. The distance and angle restraints for G_O were derived from x-ray structures of 9-ethyl-8-oxoguanine (31) obtained from the Cambridge Structural Database (32). The quality of the electron density maps can be observed in Fig. 2. Hydrogen positions were calculated with the program INSIGHTII (33).

As experienced previously with XPLOR, DNA base planarity was slightly compromised during refinement (34). To minimize this artifact, values of some planarity force constants were increased. Although these parameter modifications significantly improved base planarity, certain atoms such as C1′ of G(6) and the symmetrically related atom of G(16) remain slightly below the base plane (see Fig. 3).

RESULTS

G_O forms Watson–Crick hydrogen bonds with the opposing cytosine. Fig. 2*A* shows a sum electron density map surrounding the C·G_O base pair. The hydrogen bonds between O6 of G_O and N4 of C (2.85 Å), N1 of G_O and N3 of C (2.95 Å), and N2 of G_O and O2 of C (2.84 Å) are very similar to those of a normal C·G base pair. O8 of G_O protrudes into the DNA major groove and is not involved in hydrogen bonding interactions with the opposite C or with water molecules. The glycosidic bond of the G_O residue is in the anti conformation (χ = −53.0°). Thus the pairing scheme observed by x-ray diffraction is consistent with that observed previously by NMR (25).

DNA containing G_O is structurally similar to unmodified, B-form DNA. Superimposition of the d(CCAG$_O$CGCTGG) coordinates with those of d(CCAGGCCTGG) (Fig. 3) indicates that no major structural perturbations are induced by G_O. Only χ (O4′-C1′-N9-C4) of residue 4, which is −53.0° in d(CCAG$_O$CGCTGG) and −84.0° in d(CCAGGCCTGG), differs significantly between the two structures. The planes of G(9) and the symmetrically related G(19) in d(CCAG$_O$CGCTGG) are offset slightly from those of d(CCAGGCCTGG). In sum the structural differences are minor. The rms deviation of atomic positions of common residues in d(CCAG$_O$CGCTGG) and d(CCAGGCCTGG) is 0.27 Å.

O8 of G_O does not sterically clash with the phosphodeoxyribose backbone, suggesting that steric effects do not influence the syn/anti equilibrium of G_O in comparison to that of normal G. In Fig. 4*A* a space-filling representation of the C·G_O base pair illustrates the lack of proximity of O8 with the DNA backbone. The closest approach of O8 to the backbone occurs with the C1′ atom (2.97 Å). The only additional close contact is with the C2′ atom of the deoxyribose. As shown in Fig. 4*A*, the C2′–O8 distance (3.19 Å) is too great to be repulsive and would not influence the syn/anti equilibrium. All other distances between O8 and nonhydrogen backbone atoms are >5.0 Å. Similarly, O8 of G_O does not encounter steric hindrance with hydrogen atoms of the deoxyribose. For G_O, O8 is 2.98 Å from the C2′ hydrogen (H2′) and 3.55 Å from H1′.

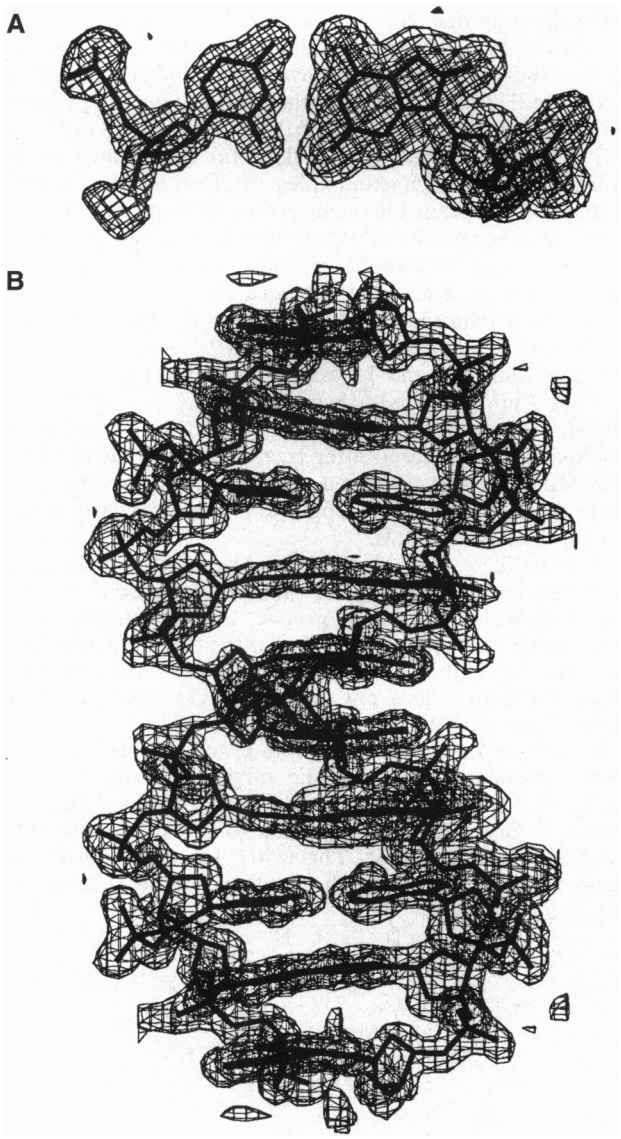

FIG. 2. Fourier sum electron density maps ($2F_o - F_c$), contoured at 1σ, surrounding the C·G_O base pair (*A*) and the complete decamer duplex (*B*).

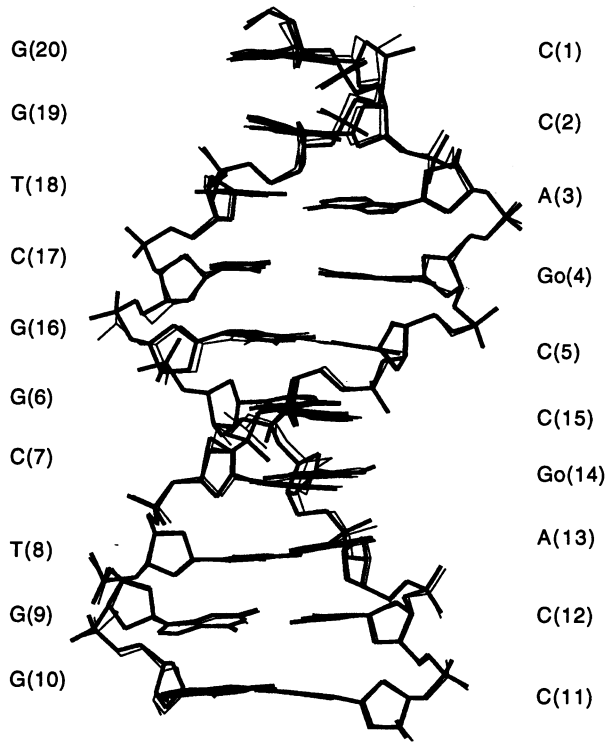

FIG. 3. Superimposition of the three-dimensional structure of d(CCAG$_O$CGCTGG) onto the previously reported (28) structure of d(CCAGGCCTGG).

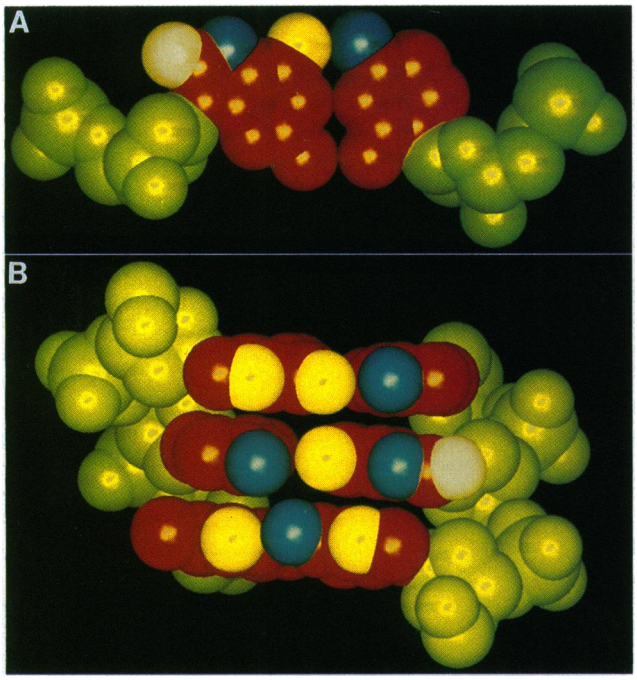

FIG. 4. (*A*) Space-filling representation of the C·G_O base pair. The bases are shown in red, with the exception of the O8 atom (white) and the hydrogen bond donors (blue) and acceptors (yellow). The sugar-phosphate backbone is green. (*B*) Space-filling representation of base pairs 3–5 of d(CCAG_OCGCTGG). The view is from the major groove, and the color coding is the same as in *A*.

The 31° difference in torsion angle χ of residue G_O(4) in d(CCAG_OCGCTGG) compared with d(CCAGGCCTGG) does not result from steric repulsion of O8 with the phospho-deoxyribose backbone. For χ of −84.0° as observed in d(CCA-GGCCTGG), the C2′–O8 distance is 3.59 Å (3.19), the H2′–O8 distance is 3.71 Å (2.98) and the H1′–O8 distance is 3.81 Å (3.55). The values in parentheses are the corresponding distances for χ of −53.0° as observed in d(CCAG_OCGCTGG). The conversion of G to G_O appears to shift χ in the opposite direction from that expected if steric repulsion of O8 with the backbone were a significant influence on conformation. Modeling studies with all possible values of χ (L.A.L. and L.D.W., unpublished work) show that the C2′–O8 distance ranges from 2.9 Å (χ = −3.0°) to 4.5 Å (χ = −186.0°), while the H2′–O8 distance ranges from 2.4 Å (χ = −7.3°) to 5.1 Å (χ = −204.3°). The H1′–O8 distance ranges from 2.5 Å (χ = 50.8°) to 4.0 Å (χ = −124.3°).

DISCUSSION

We have determined the x-ray crystal structure of a DNA fragment containing G_O. The results indicate that G_O forms Watson–Crick hydrogen bonds with the opposing cytosine and that DNA containing G_O is structurally similar to unmodified, B-form DNA.

G_O is recognized by a specific array of DNA repair enzymes. The structure described here allows us to identify probable recognition elements by which MutM distinguishes C·G_O^{anti} base pairs. Recognition of C·G_O^{anti} base pairs can be understood within a general framework of DNA sequence-specific protein recognition. As noted by Seeman *et al.* (35), each of the four normal base pairs presents a distinct pattern of hydrogen bond donors/acceptors from the major groove but not from the minor groove. For each normal and G_O-containing base pair, patterns of hydrogen bond donors/acceptors are given in Table 2, where we have used the pseudo-twofold axis of each base pair as a positional reference along the edge of a base pair.

Table 2. Hydrogen bond donors/acceptors

Base pair	Major groove	Minor groove	MutM substrate
C·G	*d*aa*	*a*da*	No
G·C	*aa*d*	*ad*a*	No
T·A	*a*da*	*a*a*	No
A·T	*ad*a*	*a*a*	No
A·G_O^{syn}	*ad*add*	*a*a*	No
T·A_O	*a*dda*	*a*a*	?
C·G_O^{anti}	*d*ada*	*a*da*	Yes
C·Fapy-G	*d*ada*	*a*da*	Yes
T·Fapy-A	*a*dda*	*a*a*	Yes

Asterisk indicates the position of the pseudo-twofold axis. The hydrogen bond donors/acceptors that are common to all substrates of MutM are shown in bold type.

As recognized by Grollman and coworkers (40), hydrogen bond donors/acceptors within the major groove provide a likely element by which MutM could recognize a series of substrates (see Fig. 4*B*). As shown in Table 2 the last two characters of the ***d*ada*** pattern of C·G_O^{anti} are common to all substrates of MutM. MutM has a high affinity for duplexes containing C·G_O^{anti} and T·G_O^{anti} base pairs, as well as the imidazole ring-opened purines [formamidopyridine (Fapy) derivatives] Fapy-adenine and Fapy-guanine (Fig. 5) (36–38). Each of these substrates has a hydrogen bond acceptor at the 8 position. This model explains the MutM requirement for the anti conformation of G_O. Further, because C·G_O^{anti} and T·G_O^{anti} are recognized, it is doubtful that MutM probes hydrogen bonding functionalities of the opposing residue. Perhaps MutM scans the major groove with an asparagine or glutamine, recognizing substrates that accept a hydrogen bond to the 8 position. Glutamine-258 and -268, possible candidates for this type of interaction, are located within a zinc finger motif that is required for MutM binding to DNA (38, 41).

Like G_O, 7,8-dihydro-8-oxoadenine (A_O) contains a hydrogen bond donor at the 7 position and an acceptor at the 8 position. At present it is unclear whether A_O^{anti} is a substrate for MutM. Boiteux *et al.* (37) observed small but detectable amounts of A_O released after treatment of irradiated DNA with MutM. However, Tchou *et al.* (16) reported that oligonucleotides containing A_O opposite any pairing partner were not substrates for MutM.

It is unlikely that MutM recognizes either a distorted conformational state of DNA or hydrogen bond donors/acceptors within the minor groove. DNA containing C·G_O base pairs is conformationally similar to normal, B-form DNA (see Fig. 3). Within the minor groove, the arrangement of donors/acceptors does not distinguish G_O base pairs from normal base pairs (see Table 2).

We believe that conversion from G to G_O does not significantly influence the glycosidic torsion preference of the nucleoside. It has been suggested (23–25, 39) that conversion from G to G_O switches the glycosidic torsion preference of the nucleoside from anti to syn. This switch is thought to arise from steric repulsion of O8 with the deoxyribose. Uesugi and

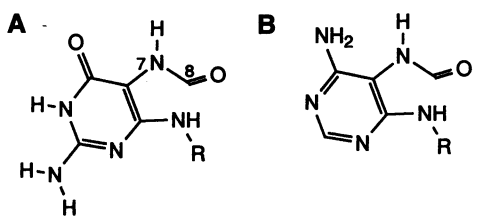

FIG. 5. Imidazole ring-opened purines that are substrates for MutM. (*A*) Fapy-guanine (2,6-diamino-4-hydroxy-5-formamidopyrimidine). (*B*) Fapy-adenine (4,6-diamino-5-formamidopyrimidine).

Ikehara (39) provided indirect experimental support for this hypothesis by comparing ^{13}C NMR chemical shifts of a series of 8-substituted guanosine derivatives including G_O. An upfield position of the C2′ resonance was considered evidence for preference of the syn conformation. This upfield shift was proposed to arise via through-space interactions of the lone pair of electrons of N3 of G with the deoxyribose. In general this through-space interaction would be specific for the syn conformation. We believe, however, that in the case of G_O this assumption may be incorrect. Modeling studies show that the location of N3 in the syn conformation is nearly the same as the location of O8 in the anti conformation (L.A.L. and L.D.W., unpublished work). A lone pair of O8 in the anti conformation should induce an upfield shift similar to that induced by N3 in the syn conformation. Thus, without switching away from the anti conformation, the ^{13}C C2′ resonance would be expected to shift upfield upon conversion of G to G_O. Furthermore, the van der Waals radius of the 8 substituent of G_O is small compared with those of other derivatives examined, suggesting that steric interactions are less significant. In the structure described here, there is no steric interaction of O_8 of G_O with the phospho-deoxyribose backbone.

It is likely that hydrogen bonds, not steric repulsion, dictate the syn/anti equilibrium of both G and G_O in DNA. Base pairing freezes the conformation in syn or anti, depending upon the pairing partner. C forms a stable base pair with G^{anti} and $G_O{}^{anti}$. However, A forms a stable base pair with $G_O{}^{syn}$. When G_O is in the syn, but not anti, conformation it mimics T and forms two hydrogen bonds with A (Fig. 1*C*). The stability of this pairing scheme probably contributes to the significant mutagenic potential of G_O.

Note Added in Proof. A recent paper (42) describes crystallographic evidence of a DNA dodecamer containing G_O opposite A.

We thank Drs. Paul Doetsch, Arthur Grollman, and Stephen Quirk for helpful discussions. This work was supported by the American Cancer Society (Grant NP-831 to L.D.W.) and the National Institutes of Health (Grant CA52127 to J.M.E.).

1. Epe, B. (1991) *Chem. Biol. Interact.* **80,** 239–260.
2. Fiala, E. S., Nie, G., Sodum, R., Conaway, C. C. & Sohn, O. S. (1993) *Cancer Lett.* **74,** 9–14.
3. Fuciarelli, A. F., Wegher, B. J., Blakely, W. F. & Dizdaroglu, M. (1990) *Int. J. Radiat. Biol.* **58,** 397–415.
4. Pflaum, M., Boiteux, S. & Epe, B. (1994) *Carcinogenesis* **15,** 297–300.
5. Michaels, M. L. & Miller, J. H. (1992) *J. Bacteriol.* **174,** 6321–6325.
6. Grollman, A. P. & Moriya, M. (1993) *Trends Genet.* **9,** 246–249.
7. Park, E. M., Shigenaga, M. K., Degan, P., Korn, T. S., Kitzler, J. W., Wehr, C. M., Kolachana, P. & Ames, B. N. (1992) *Proc. Natl. Acad. Sci. USA* **89,** 3375–3379.
8. Wood, M. L., Dizdaroglu, M., Gajewski, E. & Essigmann, J. M. (1990) *Biochemistry* **29,** 7024–7032.
9. Shibutani, S., Takeshita, M. & Grollman, A. P. (1991) *Nature (London)* **349,** 431–434.
10. Pavlov, Y. I., Minnick, D. T., Izuta, S. & Kunkel, T. A. (1994) *Biochemistry* **33,** 4695–4701.
11. Bhatnagar, S. K., Bullions, L. C. & Bessman, M. J. (1991) *J. Biol. Chem.* **266,** 9050–9054.
12. Maki, H. & Sekiguchi, M. (1992) *Nature (London)* **355,** 273–275.
13. Michaels, M. L., Tchou, J., Grollman, A. P. & Miller, J. H. (1992) *Biochemistry* **31,** 10964–10968.
14. Michaels, M. L., Pham, L., Cruz, C. & Miller, J. H. (1991) *Nucleic Acids Res.* **19,** 3629–3632.
15. Bessho, T., Roy, R., Yamamoto, K., Kasai, H., Nishimura, S., Tano, K. & Mitra, S. (1993) *Proc. Natl. Acad. Sci., USA* **90,** 8901–8904.
16. Tchou, J., Kasai, H., Shibutani, S., Chung, M.-H., Laval, J., Grollman, A. P. & Nishimura, S. (1991) *Proc. Natl. Acad. Sci. USA* **88,** 4690–4694.
17. Michaels, M. L., Pham, L., Nghiem, Y., Cruz, C. & Miller, J. H. (1990) *Nucleic Acids Res.* **18,** 3841–3845.
18. Michaels, M. L., Cruz, C., Grollman, A. P. & Miller, J. H. (1992) *Proc. Natl. Acad. Sci. USA* **89,** 7022–7025.
19. Moriya, M. & Grollman, A. P. (1993) *Mol. Gen. Genet.* **239,** 72–76.
20. Vidmar, J. J. & Cupples, C. G. (1993) *Can. J. Microbiol.* **39,** 892–894.
21. Mo, J. Y., Maki, H. & Sekiguchi, M. (1992) *Proc. Natl. Acad. Sci. USA* **89,** 11021–11025.
22. Bessho, T., Tano, K., Kasai, H., Ohtsuka, E. & Nishimura, S. (1993) *J. Biol. Chem.* **268,** 19416–19421.
23. Cho, B. P. & Evans, F. E. (1991) *Nucleic Acids Res.* **19,** 1041–1047.
24. Kouchakdjian, M., Bodepudi, V., Shibutani, S., Eisenberg, M., Johnson, F., Grollman, A. P. & Patel, D. J. (1991) *Biochemistry* **30,** 1403–1412.
25. Oda, Y., Uesugi, S., Ikehara, M., Nishimura, S., Kawase, Y., Ishikawa, H., Inoue, H. & Ohtsuka, E. (1991) *Nucleic Acids Res.* **19,** 1407–1412.
26. Lin, T.-S., Cheng, J.-C., Ishiguro, K. & Sartorelli, A. C. (1985) *J. Med. Chem.* **28,** 1194–1198.
27. Wood, M. L., Esteve, A., Morningstar, M. L., Kuziemko, G. M. & Essigmann, J. M. (1992) *Nucleic Acids Res.* **20,** 6023–6032.
28. Heinemann, U. & Alings, C. (1989) *J. Mol. Biol.* **210,** 369–381.
29. Sack, J. (1990) *Chain: A Crystallographic Modelling Program* (Baylor College of Medicine, Waco, TX).
30. Brunger, A. (1988) XPLOR Software (Howard Hughes Med. Inst., Yale Univ., New Haven, CT).
31. Doi, M., In, Y., Kikuchi, M., Ishida, T. & Inoue, M. (1991) *J. Chem. Soc., Perkin Trans. 1* **55,** 55–61.
32. Allen, F. H., Davies, J. E., Galloy, J. J., Johnson, O., Kennard, O., Macrae, C. F., Mitchell, E. M., Mitchell, G. F., Smith, J. M. & Watson, D. G. (1991) *J. Chem. Info. Comp. Sci.* **31,** 187–204.
33. Biosym Technologies (1991) INSIGHTII (Biosym Technologies, San Diego).
34. Hahn, M. & Heinemann, U. (1993) *Acta Crystallogr.* **D49,** 468–477.
35. Seeman, N. C., Rosenberg, J. M. & Rich, A. (1976) *Proc. Natl. Acad. Sci. USA* **73,** 804–808.
36. Boiteux, S., O'Connor, T. R., Gajewski, E., Lederer, F., Gouyette, A. & Laval, J. (1990) *J. Biol. Chem.* **265,** 3916–3922.
37. Boiteux, S., Gajewski, E., Laval, J. & Dizdaroglu, M. (1992) *Biochemistry* **31,** 106–110.
38. Castaing, B., Geiger, A., Seliger, H., Nehls, P., Laval, J., Zelwer, C. & Boiteux, S. (1993) *Nucleic Acids Res.* **21,** 2899–2905.
39. Uesugi, S. & Ikehara, M. (1977) *J. Am. Chem. Soc.* **99,** 3250–3253.
40. Tchou, J., Bodepudi, V., Shibutani, S., Antoshechkin, I., Miller, J., Grollman, A, P. & Johnson, F. (1994) *J. Biol. Chem.* **269,** 15318–15324.
41. Tchou, J., Michaels, M. L., Miller, J. H. & Grollman, A, P. (1993) *J. Biol. Chem.* **268,** 26738–26744.
42. McAuley-Hecht, K. E., Leonard, G. A., Gibson, N. J., Thomson, J. B., Watson, W. P., Hunter, W. N. & Brown, T. (1994) *Biochemistry* **33,** 10266–10270.